Journal of Cell Science 111, 2885-2895 (1998)
Printed in Great Britain © The Company of Biologists Limited 1998
JCS7277

Muscle-specific functions of ryanodine receptor channels in *Caenorhabditis elegans*

Ed B. Maryon*, Bonnie Saari and Philip Anderson

Department of Genetics, University of Wisconsin, Madison, Wisconsin 53706, USA
*Author for correspondence (e-mail: ebmaryon@facstaff.wisc.edu)

Accepted 16 July; published on WWW 9 September 1998

SUMMARY

Ryanodine receptor channels regulate contraction of striated muscle by gating the release of calcium ions from the sarcoplasmic reticulum. Ryanodine receptors are expressed in excitable and non-excitable cells of numerous species, including the nematode *C. elegans*. Unlike vertebrates, which have at least three ryanodine receptor genes, *C. elegans* has a single gene encoded by the *unc-68* locus. We show that *unc-68* is expressed in most muscle cells, and that the phenotypic defects exhibited by *unc-68* null mutants result from the loss of *unc-68* function in pharyngeal and body-wall muscle cells. The loss of *unc-68* function in the isthmus and terminal bulb muscles of the pharynx causes a reduction in growth rate and brood size. *unc-68* null mutants exhibit defective pharyngeal pumping (feeding) and have abnormal vacuoles in the terminal bulb of the pharynx. *unc-68* is required in body-wall muscle cells for normal motility. We show that UNC-68 is localized in body-wall muscle cells to flattened vesicular sacs positioned between the apical plasma membrane and the myofilament lattice. In *unc-68* mutants, the vesicles are enlarged and densely stained. The flattened vesicles in body-wall muscle cells thus represent the *C. elegans* sarcoplasmic reticulum. Morphological and behavioral phenotypes of *unc-68* mutants suggest that intracellular calcium release is not essential for excitation-contraction coupling in *C. elegans*.

Key words: Ryanodine receptor, E-C coupling, Calcium, Sarcoplasmic reticulum

INTRODUCTION

Ryanodine receptors (RyRs) are intracellular ion channels that gate the release of calcium ions (Ca^{2+}) from internal stores (Coronado et al., 1994). The channels are ubiquitous in metazoans and may also be present in plants (Sutko and Airey, 1996; Muir and Sanders, 1996). In striated muscle, RyR channels and voltage gated Ca^{2+} channels (VGCC) in the plasma membrane mediate excitation-contraction coupling (E-C coupling). Contraction is preceded by a massive release of stored Ca^{2+} through RyR channels, which open in response to activation of VGCCs (Caterall, 1991). RyRs are located in membranes of the sarcoplasmic reticulum (SR), a specialized endoplasmic reticulum surrounding muscle fibers (Franzini-Armstrong and Protasi, 1997). RyRs cluster in junctions between the SR and the surface membrane or invaginations of the surface membrane called T-tubules (Block et al., 1996). Vertebrate RyRs have also been characterized in a variety of other cell types, but the biological role the channels play in non-muscle cells is poorly understood (Bennett et al., 1996).

Vertebrates have three known RyR genes, encoding predicted proteins of approximately 5,000 amino acids (≈565 kDa). A hydrophobic domain within the carboxyl-terminal 600 amino acids contains the channel pore and the binding site for ryanodine, a plant alkaloid that locks open RyRs and induces contractile paralysis of striated muscle (Bhat et al., 1997; Callaway et al., 1994). Functional channels are homotetramers. The large (2.24 million Da) RyR channels are visible in EM sections of skeletal muscle triad junctions as 'feet' that span the gap between the SR and T-tubule membranes (Block et al., 1996; Wagenknecht and Radermacher, 1995).

The three vertebrate RyR isoforms (RyR-1-RyR-3) have different expression patterns and gating mechanisms (Sutko and Airey, 1996). RyR-1 channels are abundant in skeletal muscle, where they are connected by direct or indirect protein-protein interactions to VGCCs (Block et al., 1996). Ca^{2+} release by RyR-1 channels is closely linked to gating charge movement in VGCCs, presumably because the two channels are coupled (Rios et al., 1991). Genetic disruption of the mouse RyR-1 gene causes late embryonic lethality. Homozygous mutant embryos contain disorganized skeletal muscle fibers that lack E-C coupling (Takeshima et al., 1994, 1995). RyR-2 channels are expressed in cardiac muscle and in the brain, and are gated by calcium-induced calcium release (CICR) (Fabiato, 1983). RyR-2 channels also cluster in junctions with the surface membrane or T-tubule membranes (Carl et al., 1995). The biological role of RyR-3 channels is not clear, because RyR-3 knockout mice exhibit only mild behavioral defects and have normal E-C coupling in skeletal muscle (Takeshima et al., 1996). In vertebrate skeletal and cardiac muscle, Ca^{2+} release from the SR is essential for E-C coupling (Varro et al., 1993; Takeshima et al., 1994).

We and others have characterized RyRs in the nematode *C. elegans*. In contrast to vertebrates, *C. elegans* has a single RyR

gene corresponding to the *unc-68* locus (Maryon et al., 1996). *unc-68* null mutants are viable, but exhibit defects in growth and motility. *unc-68* encodes a predicted protein of 5071 amino acids that is approximately 40% identical to each of the three mammalian RyR isoforms (Sakube et al., 1997). *unc-68* promoter-*lacZ* reporter constructs are expressed in muscle, neurons, and other cells, the pattern of expression depending on the extent of upstream sequence included (Sakube et al., 1997). Ryanodine induces contractile paralysis of wild-type *C. elegans*. Wild-type *C. elegans* homogenates contain ryanodine-binding activity which co-purifies with high-conductance, ryanodine-gated channels (Kim et al., 1992). *unc-68* null mutants lack ryanodine-binding activity and are completely resistant to the paralyzing effects of ryanodine (Maryon et al., 1996).

unc-68 mutants were originally identified as being defective in locomotion, a behavior resulting from coordinated contraction and relaxation of 95 body-wall muscle cells (Brenner, 1974; Wood, 1988). The ultrastructure of body-wall muscle is approximately normal in *unc-68* mutants, but contraction is weak and attenuated. *unc-68* mutants also exhibit defects of pharyngeal pumping, a behavior mediated by 20 pharyngeal muscle cells. In addition to visible defects in muscle function, *unc-68* mutants grow more slowly and have fewer offspring than wild type. In this report, we show that the obvious phenotypic defects exhibited by *unc-68* mutants are due to the loss of UNC-68 function in body-wall and pharyngeal muscles. We have identified the *C. elegans* SR in body-wall muscle cells as a network of vesicular membranous organelles surrounding the myofilament lattice. We show that UNC-68 is localized to surface membrane-associated vesicles that resemble junctional SR of vertebrate skeletal and cardiac muscle. The behavioral and morphological phenotypes of *unc-68* mutant animals suggest that intracellular Ca^{2+}-release is not essential for EC-coupling in *C. elegans*.

MATERIALS AND METHODS

Strains and handling of *C. elegans*

Handling of *C. elegans* was done using established methods (Wood, 1988). Strains and relevant mutations used were N2 (wild type), *unc-68*(*r1161*), *unc-68*(*r1162*), *unc-68*(*r1221*), and *unc-68*(*e540*). Motility assays were performed as previously described (Maryon et al., 1996). Brood sizes were determined by counting the total number of offspring from single hermaphrodites. Growth rates at 20°C were determined by allowing adult hermaphrodites to lay eggs for 30 minutes, after which the adults were removed. The plates were observed after 60 hours at two hour intervals until the first F_1 generation eggs were laid. The generation time was defined as the interval between the time the eggs were collected and the time F_1 progeny eggs were laid.

Clones and transformation

Cloning and manipulation of DNA was performed using standard protocols. Three clones were constructed for injection transformation experiments: (1) pEM30, in which the *unc-68* promoter is linked to the green fluorescent protein (GFP) coding sequence (Chalfie et al., 1994); (2) pEM28, in which the *myo-3* promoter is linked to exons 1-8 of the *unc-68* gene; and (3) pEM24, a derivative of pEM28 in which the GFP coding sequence (and translational start sequence) is inserted upstream of *unc-68* exons 1-8. For pEM30, *unc-68* base pairs 2,145-4,884 (which includes the first 19 amino acids of UNC-68 and 2.6 kb of upstream sequence) was amplified by PCR from N2 genomic DNA and inserted into *Xba*I + *Age*I-digested pPD95.69 (a GFP expression vector; Fire et al., 1990). pEM28 is derived from pPD96.52, an 'ectopic' expression vector containing the *myo-3* promoter (Fire et al., 1990). A synthetic fragment having the first 22 amino acids of UNC-68 (the 20 amino acids from exon 1 and the first 2 amino acids from exon 2) was ligated to a PCR fragment amplified from genomic DNA containing exons 2-8 (*unc-68* base pairs 8,968-11,804), and inserted into *Kpn*I + *Apa*I-digested pPD96.52. pEM28 also contains an engineered *Not*I site which changes the predicted UNC-68 amino-terminal protein sequence from MADKEE to MRPHKEE. pEM24 was constructed by ligating the GFP coding sequence and translational start (amplified from the GFP vector pPD 95.81) into *Kpn*I + *Not*I cut pEM28. All junctions created during construction of pEM24, pEM28, and pEM30 were verified by sequencing. No PCR-induced mutations were found in *unc-68* exons 2-8 of pEM28.

Transformation rescue

Adult wild-type or *unc-68* hermaphrodites were microinjected as previously described (Maryon et al., 1996). DNA fragments used in rescue experiments were amplified from N2 genomic DNA as described (Maryon et al., 1996). DNA from five or more separate reactions was pooled for each fragment to minimize the contribution of PCR-induced mutations. The amplified *unc-68* fragments and cloned constructs were injected at a concentration of 20 μg/ml. Carrier DNA (*Pvu*II-digested N2 genomic DNA) was included in all injections at a concentration of 80 μg/ml. Four to ten independent transformants were obtained for each fragment mixture. The *unc-68* promoter-GFP construct pEM30 was coinjected with pRF4, a clone expressing a dominant *rol-6* allele that allows transformed animals to be identified (Mello and Fire, 1995). Rescued *unc-68* animals were identified by screening progeny of injected *unc-68* hermaphrodites for animals with wild-type motility.

Antibodies

Polyclonal anti-UNC-68 antibodies were raised in rabbits and rats by immunizing and boosting the animals with a gel-purified bacterially-expressed UNC-68::GST fusion protein (pGEX4T-1 vector; Pharmacia Biotech Piscataway NJ) that includes amino acids 3,429-3,812 of the predicted UNC-68 protein (Sakube et al., 1997). Whole sera was affinity purified by absorption to a column prepared with a histidine-tagged fusion protein (pET-28a(+); Novagen, Inc. Madison, WI) containing UNC-68 amino acids 3,429-3,812. Eluted antibody was then absorbed sequentially to affinity columns made with: (1) total proteins from bacteria transformed with pGEX4T-1, and (2) total proteins from *unc-68(r1161). r1161* is a 7.2 kb deletion that removes the UNC-68 amino acids in the fusion protein (Maryon et al., 1996). Mouse monoclonal antibodies specific for vinculin (MH24) and alpha-actinin (MH35) were kindly provided by Michelle Hresko and Ross Francis. Mouse monoclonals specific for UNC-54 (myosin heavy chain B) and MYO-C (pharyngeal myosin) were kindly provided by David Miller. Oregon Green™- or Cy™3-conjugated secondary antibodies were from Molecular Probes (Eugene OR) and Jackson Immunoresearch Labs (West Grove, PA), respectively.

Western analysis

Microsomal preparations enriched for UNC-68 were purified from whole worm homogenates as previously described (Maryon et al., 1996). Microsomal proteins were fractionated on 4-12% gradient SDS-PAGE gels, then transferred to membranes as described (Seok et al., 1992). Chemoluminescence detection was performed with the ECL™ detection system (Amersham Life Science, Cleveland, OH) as recommended by the manufacturer.

Microscopy

Mixed stage populations of wild-type and *unc-68* mutant animals were fixed, stained and mounted as described ('whole-mount fixation

of larvae and adults' in Miller and Shakes, 1995), with some modifications: (1) the 'Ruvken' fixation buffer did not include methanol; (2) the incubation in 1% β-mercaptoethanol was replaced by three 5 minute washes in 5% β-mercaptoethanol and one 10 minute wash in 5% β-mercaptoethanol + 200 μg/ml proteinase K; (3) the final wash in BO_3 buffer was followed by a 10 minute fix in Ruvken buffer and two 5 minute washes in PBSTw (see Miller and Shakes, 1995). The specimens were then incubated 10 minutes in −20°C methanol, followed by rehydration through a 75%, 50%, 25% methanol:PBSTw series. Living specimens were anesthetized in 0.25% sodium azide and mounted on agar pads. Light and epi-fluorescent micrographs were taken using a Zeiss Axioskop microscope. Confocal images were collected with a Bio-Rad 1024 instrument. For transmission electron microscopy, animals were fixed, sectioned, and mounted on grids and stained as previously described (Maryon et al., 1996). Transverse sections (70 nm thick) were viewed and photographed with a Philips 410 electron microscope at ×14,500 (Fig. 9) and ×65,000 (Fig. 10).

RESULTS

Tissues of *unc-68* expression

We identified cells that express *unc-68* by fusing the *unc-68* promoter to a reporter gene and transforming wild-type *C. elegans* with the construct. The *unc-68* promoter (including 2,590 bp of upstream genomic DNA) and the first 18 amino acids of exon #1 (Sakube et al., 1997) was amplified from wild-type genomic DNA and inserted into a green fluorescent protein (GFP) expression vector (Chalfie et al., 1994; Fire et al., 1990). The resulting construct (pEM30) was microinjected injected into wild-type hermaphrodites, and stably transformed animals were identified among the progeny. As shown in Fig. 1, GFP fluorescence is observed in several muscle cell types of the transformants, including body-wall muscle cells (Fig. 1A), terminal bulb muscles of the pharynx (Fig. 1B, large arrow), vulval and uterine muscle (involved in egg-laying; Fig. 1C), diagonal muscles of the male tail (used for mating; Fig. 1D), the anal sphincter muscle (Fig. 1E, arrow), and anal depressor muscles (Fig. 1E, arrowhead). GFP expression is variably observed in unidentified neurons in the head (e.g. Fig. 1B, arrowhead). We first observe GFP expression in body-wall and pharyngeal muscle cells in 11/2-fold embryos, approximately the time when twitching of embryonic body wall muscles begins (Williams and Waterston, 1994; Fig. 1F). The corpus muscles of the pharynx did not express GFP (Fig. 1B, small arrow).

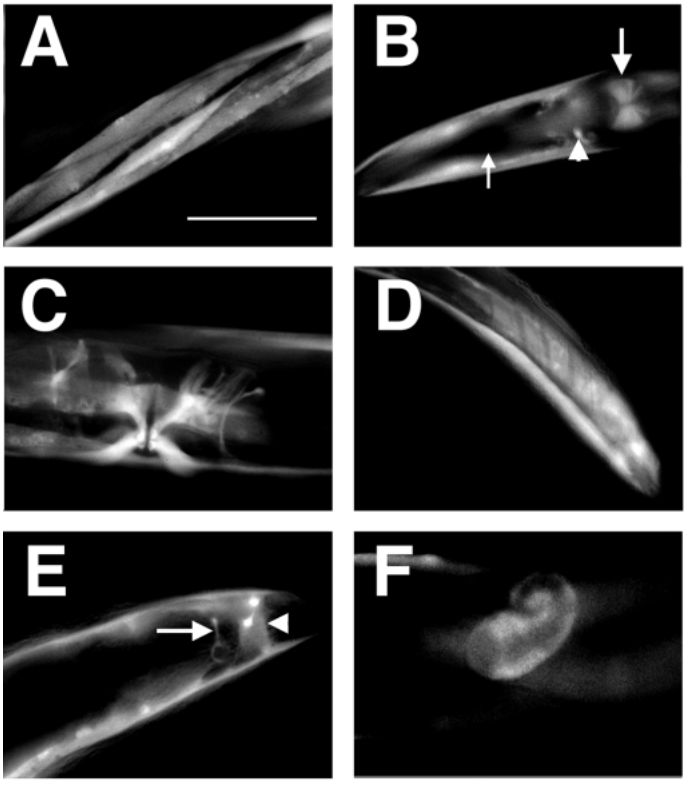

Fig. 1. Expression of an *unc-68* promoter:GFP reporter construct in wild-type animals (A) GFP fluorescence in two body-wall muscle quadrants. (B) GFP expression in the head. Large arrow: terminal bulb of the pharynx. Arrowhead: expression in an unidentified neuron of the nerve ring. The small arrow points to the corpus muscles of the pharynx, which do not express GFP. (C) GFP expression in vulval muscles and uterine muscles. (D) GFP signal in diagonal muscles of the male tail. (E) GFP expression in the anal sphincter (arrow) and anal depressor muscles (arrowhead). (F) GFP expression in a one and one-half fold elongating embryo. Bar, 50 μm.

Rescue of *unc-68* cell-specific phenotypic defects

We used transformation rescue with an ectopic promoter to assign *unc-68* mutant defects to the loss of *unc-68* function in specific muscle cells. *unc-68* null mutants exhibit multiple phenotypes, including reduced motility, insensitivity to ryanodine, abnormal pharyngeal pumping, male mating defects, and slow growth. The motility defect suggests that *unc-68* function is required in body-wall muscle. The reduced brood size and slower growth rate could be due to reduced feeding caused by defective pharyngeal pumping, to impaired motility, or to loss of function in egg-laying and/or enteric muscles. We rescued *unc-68* null mutants with the *unc-68* gene transcribed by its natural promoter or by the *myo-3* promoter. *myo-3* encodes myosin heavy chain A, a thick filament protein expressed in body-wall muscle, enteric muscle, vulval muscles of the hermaphrodite, and diagonal muscles of the male tail (Moerman and Fire, 1997). *myo-3* is not expressed in pharyngeal muscle cells, which express pharyngeal-specific myosin isoforms (Moerman and Fire, 1997).

To rescue *unc-68* mutant animals, we injected overlapping PCR fragments amplified from genomic DNA that span the *unc-68* gene (see Fig. 2A). The fragments recombine by homologous recombination in the hermaphrodite gonad to reconstruct intact *unc-68* genes (Maryon et al., 1996). Three fragment mixtures were used for transformation (see Fig. 2A). First, animals were injected with three wild-type fragments. Second, the promoter-containing fragment was replaced with a cloned construct in which the *myo-3* promoter was fused to exons 1-8 of *unc-68* (pEM28). Third, the pEM28 fragment was exchanged with a derivative in which the GFP protein was added to the amino terminus of the *unc-68* coding sequence (pEM24). As shown in Fig. 2B, transformants obtained using the *unc-68* promoter and *myo-3* promoter fragments exhibited wild-type motility and sensitivity to ryanodine. Males rescued with the *unc-68* or *myo-3* promoter constructs mate normally, showing that *unc-68* expression is required in either body-wall muscles or male tail muscles (or both) for male mating.

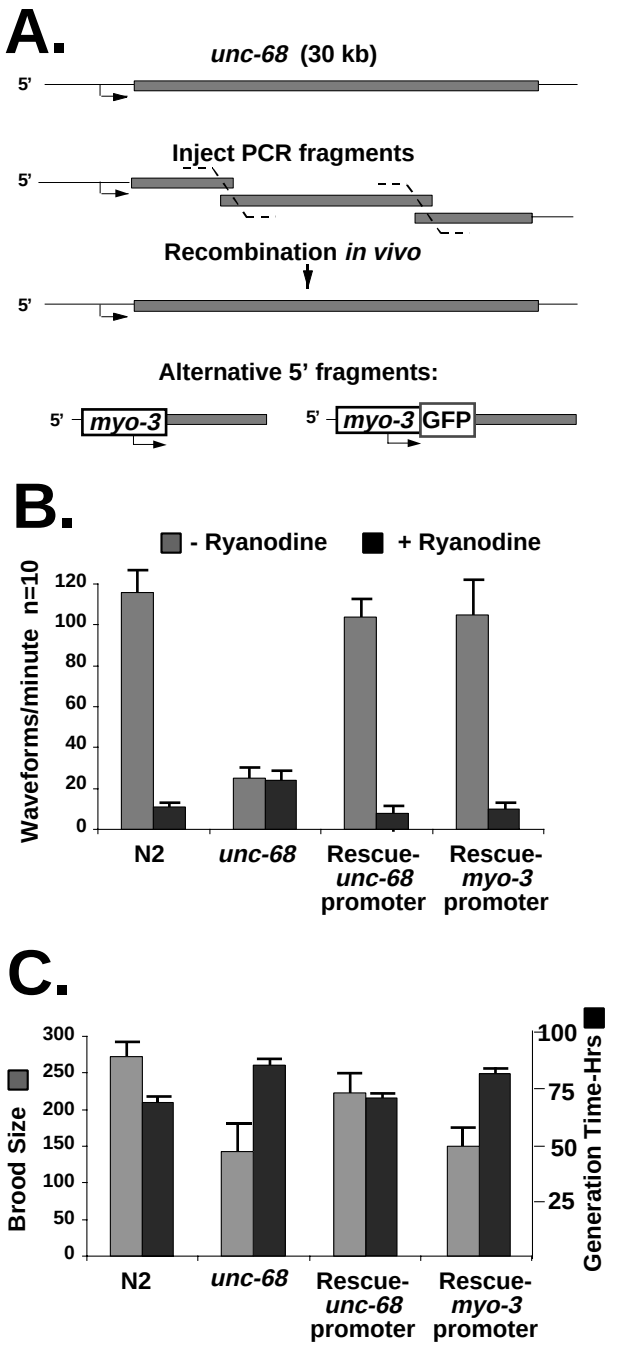

Fig. 2. Phenotypes of wild-type, *unc-68* mutant, and Unc-68(+) transformants. (A) Transformation rescue with the *unc-68* gene. Overlapping PCR fragments recombine in the hermaphrodite gonad to create intact *unc-68* genes. The alternative 5′ fragments shown create genes transcribed by the *myo-3* promoter. (B) Motility assays in liquid medium. The number of waveforms propagated in one minute (with or without 1 mM ryanodine) was averaged (error bar = s.d., n=10). (C) Left axis. Brood size; broods from at least 10 animals of the indicated strains were averaged. The differences between the brood sizes of N2 (wild-type) and either *unc-68* mutant or animals rescued with the *myo-3* promoter were statistically significant (P<.001, Student's t-test). Right axis. Generation times at 20°C of the indicated strains, n=3, error bar = s.d. (see Materials and Methods).

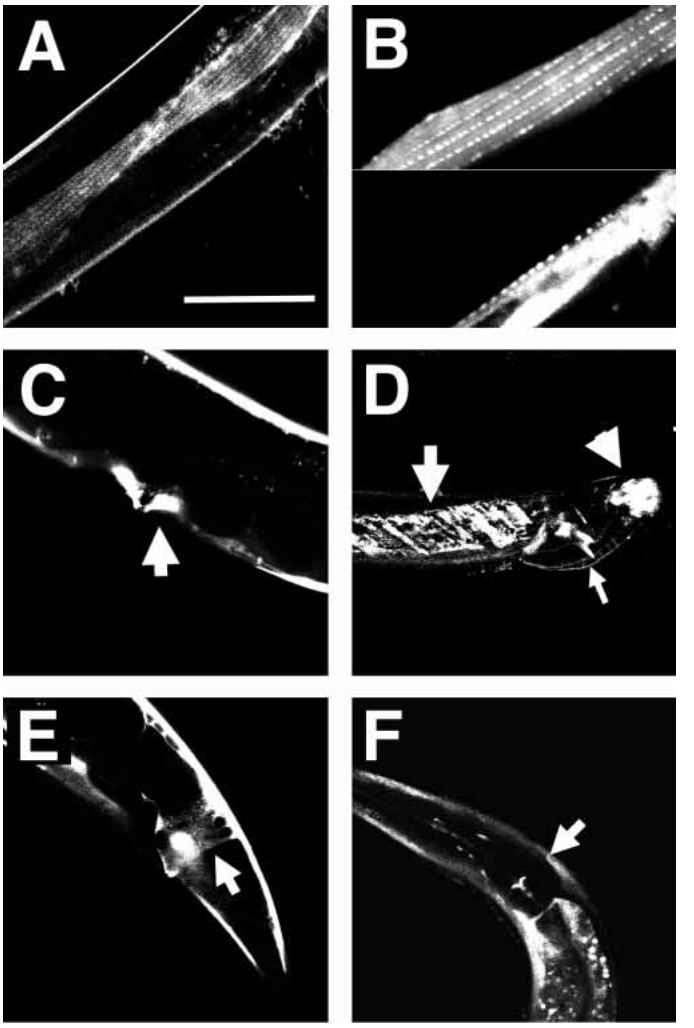

Fig. 3. GFP fluorescence in *unc-68* mutants rescued with transgenes expressing GFP::UNC-68 from the *myo-3* promoter. (A) GFP::UNC-68 expression in cells from one quadrant of body-wall muscle. (B) A single body-wall muscle cell viewed parallel (above) or perpendicular (below) to the plane of the apical plasma membrane. (C) Expression in vulval muscles, arrow shows two muscle cells. (D) GFP::UNC-68 Expression in male tail diagonal muscles (large arrow), in the spicule protractor (small arrow), and in the posterior oblique muscles (arrowhead). (E) GFP::UNC-68 expression in the anal depressor and anal sphincter muscles. (F) Absence of GFP::UNC-68 expression in the pharynx. The arrow points to the terminal bulb, which exhibits only background fluorescence inside the lumen. Bar, 50 μm.

Transformants obtained using the *unc-68* promoter exhibit generation times and brood sizes comparable to wild-type (Fig. 2C), while those obtained using the *myo-3* promoter exhibit generation times and brood sizes comparable to *unc-68* null mutants. We conclude that *unc-68* function is required in body-wall muscles for normal locomotion, and appears to be required pharyngeal muscles for wild-type brood size and generation time. The pharyngeal muscle defects in *unc-68* null mutants presumably impair feeding, thus causing slow growth and reduced fecundity (see Avery, 1993; Avery and Thomas, 1997).

As expected, transformants obtained with pEM24 (which contains the myo-3 promoter) express GFP::UNC-68 in body-wall muscles, visible as rows of obliquely striated punctate fluorescence in or near the myofilament lattice. (Fig. 3A,B). GFP::UNC-68 is also expressed in vulval muscles (Fig. 3C), diagonal muscles, spicule protractor and posterior oblique muscles of the male tail (Fig. 3D), and enteric muscles (Fig. 3E). GFP::UNC-68 is not detected in the pharynx (Fig. 3F). Like transformants obtained using pEM28, pEM24 transformants exhibit normal motility, but grow slowly and have reduced brood sizes (not shown). The expression pattern of GFP:UNC-68 in pEM24 transformants confirms that the reduction in fecundity and growth rate is correlated with a loss of *unc-68* function in the pharynx, rather than in egg-laying or enteric muscles. Furthermore, egg-laying and defecation is grossly normal in *unc-68* mutants (see Maryon et al., 1996).

Pharyngeal abnormalities in *unc-68* mutants

Defective pharyngeal muscle function in *unc-68* mutants is accompanied by abnormal vacuole-like structures in the terminal bulb of the pharynx. When *unc-68* mutant animals are viewed with Nomarski optics, the vacuoles give the terminal bulb a pitted appearance (Fig. 4B). Unc-68(+) motile transformants rescued with the wild-type *unc-68* gene have normal looking terminal bulbs (compare Fig. 4C to A), while those rescued with *unc-68* expressed from the *myo-3* promoter have the same pitted appearance as do *unc-68* mutant animals (Fig. 4D). These data show that the terminal bulb vacuoles are correlated with the loss of *unc-68* expression in the pharynx.

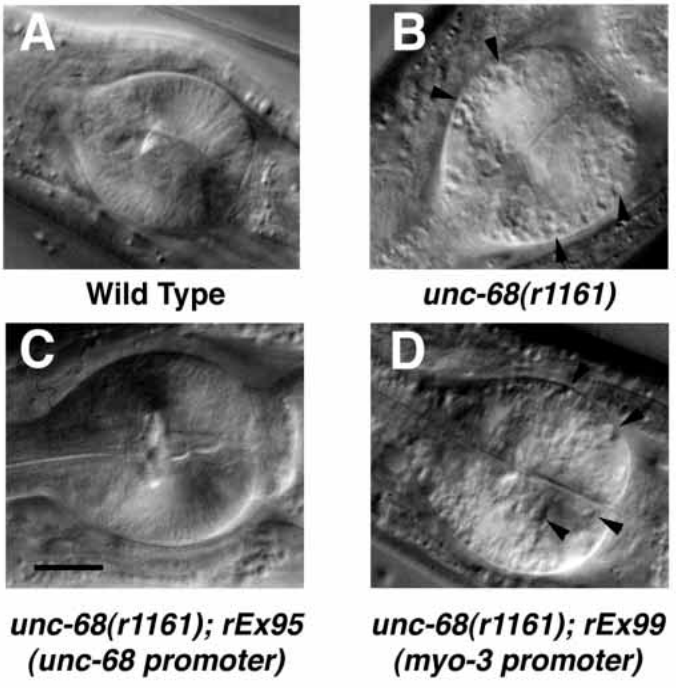

Fig. 4. Nomarski images of pharyngeal terminal bulbs. (A) Wild type. (B) *unc-68* (*r1161*), (arrowheads in B and D show vacuole-like structures that give the terminal bulb a 'pitted' appearance). (C) Unc-68(+) motile transformant rescued with the wild-type *unc-68* gene. (D) Unc-68(+) motile transformant rescued with a construct in which *unc-68* is expressed by the *myo-3* promoter. Bar, 10 μm.

Localization of UNC-68

To localize UNC-68 in situ we raised rabbit and rat polyclonal antibodies against UNC-68 fusion proteins. Affinity-purified anti-UNC-68 antibodies identified high molecular weight polypeptides on western blots of *C. elegans* microsomal

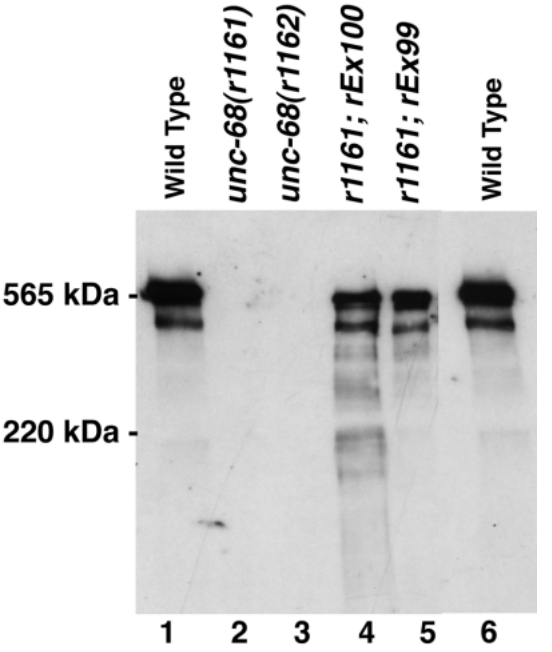

Fig. 5. Western analysis of microsomal proteins. Microsomal fractions were separated in a 4-12% SDS-PAGE gradient gel, and incubated with anti-UNC-68 polyclonal antibodies. The positions of myosin (220 kDa), and rabbit skeletal RyR (565 kDa) are shown at left. Microsomes from: wild type (lanes 1 and 6). *unc-68(r1161)* (lane 2) and *unc-68(r1162)* (lane 3) *unc-68(r1162)::rEx95* (lane 4), *unc-68(r1162)::rEx100* (lane 5).

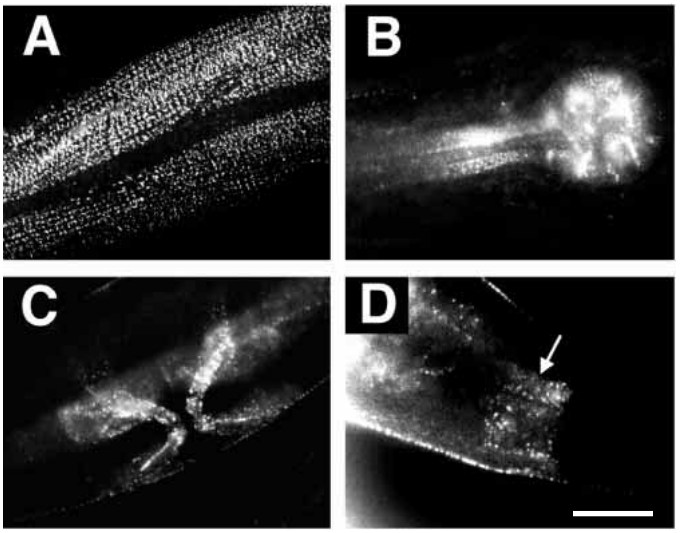

Fig. 6. Immunofluorescent staining with anti-UNC-68 in wild-type *C. elegans*. (A) Staining in body-wall muscles. (B) Staining in the posterior isthmus and terminal bulb in the pharynx. (C) Staining in vulval muscles. (D) Staining of the anal depressor muscle. Bar, 20 μm.

proteins. All immunoreactive polypeptides are absent in *unc-68* null mutants (Fig. 5). The slowest migrating, most prominent bands in Fig. 5 represent intact UNC-68. The more rapidly migrating species, which vary in intensity between preparations, are most likely proteolytic products of the larger protein. It is also possible that the smaller polypeptides are products of alternative transcripts. Microsomes from animals rescued with either the wild-type *unc-68* gene (lane 4) or the construct in which *unc-68* is expressed form the *myo-3* promoter (lane 5) contain the same polypeptides seen in wild type.

We stained fixed, whole mount animals with anti-UNC-68 antibodies (Miller and Shakes, 1995). We observe punctate staining in body-wall muscle cells, in the isthmus and terminal bulb of the pharynx, in vulval muscles and in enteric muscles (see Fig. 6A-D). Staining of body-wall muscle outlines the spindle region of muscle cells (Fig. 6A). In the pharynx, the posterior half of the isthmus muscles and the terminal bulb muscles are stained (Fig. 6B). Vulval and enteric muscles are also stained (Fig. 6C,D). Diagonal muscles of the male tail were poorly stained (not shown), probably because our whole-mount fixation protocol damaged male tails. The anti-UNC-68 antibodies, therefore, stained most, but not all of the cells that expressed the *unc-68* promoter:GFP reporter construct (see Fig. 1). We did not detect UNC-68 in neurons of the nerve ring or the anal sphincter muscle. It is possible that these or other cells express UNC-68 at levels too low to be detected with in situ immunofluorescence. Alternatively, *unc-68* reporter constructs may be expressed inappropriately in some cells.

To further localize UNC-68 channels within muscle cells, we stained animals with both anti-UNC-68 antibodies and monoclonal antibodies specific for proteins found in pharyngeal and/or body-wall muscle. Vinculin is a component of the basement membrane surrounding the pharynx (Moerman and Fire, 1997). Fig. 7A shows staining of pharyngeal and head muscles with anti-UNC-68 (green), and anti-vinculin (red). All

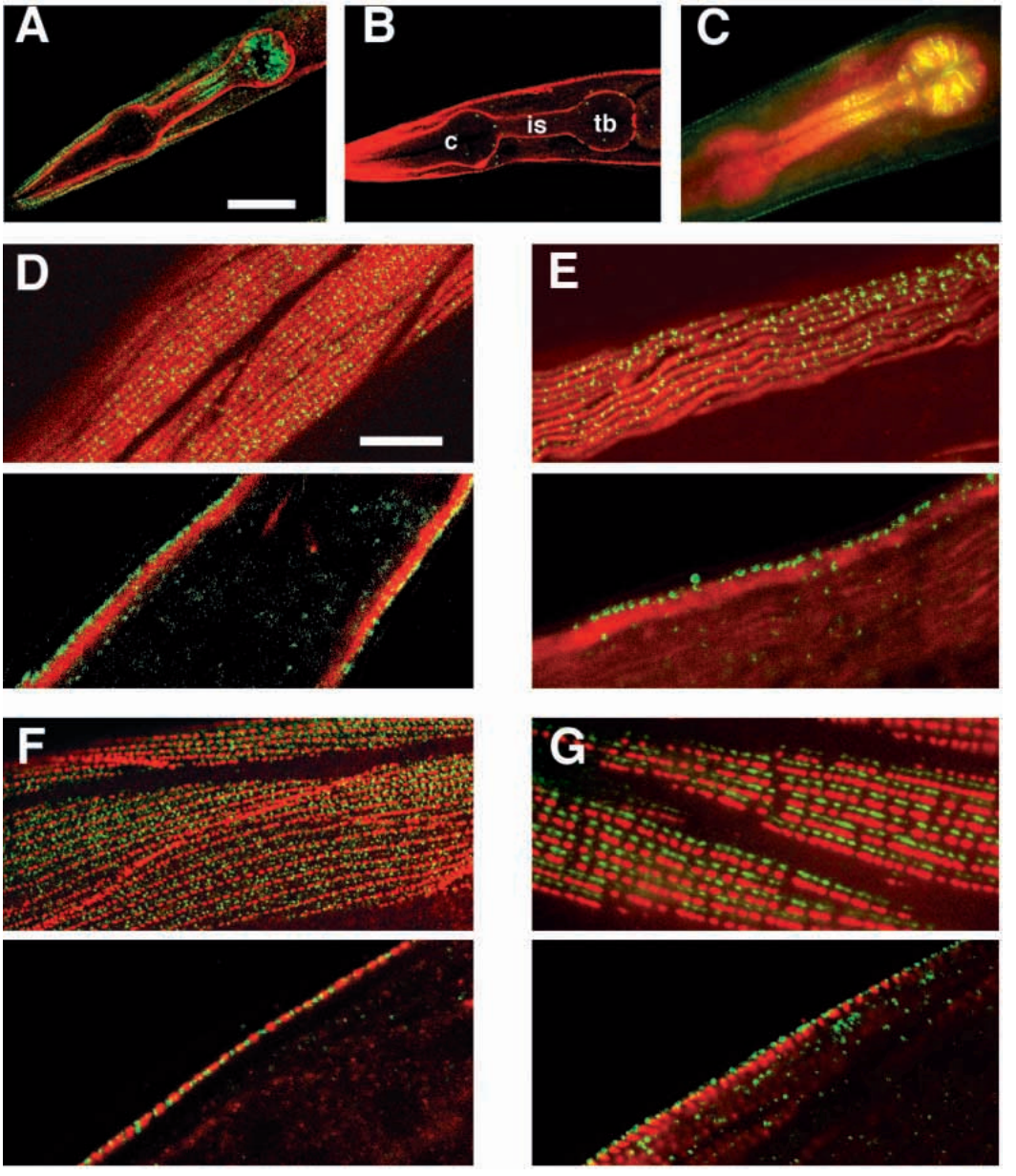

Fig. 7. Double labeling with anti-UNC-68 polyclonal antibodies and monoclonal antibodies specific for myofilament lattice proteins. In each panel, anti-UNC-68 antibody staining is shown in green/yellow, and myofilament lattice antibody staining is shown in red. (A) Staining of wild-type pharynx with anti-vinculin and anti UNC-68 (bar, 50 μm). (B) Staining of *unc-68(r1161)* mutant pharynx with anti-vinculin and anti-UNC-68. The corpus (c), isthmus (is), and terminal bulb (tb) are indicated. (C) Wild-type pharynx stained with anti-MYO-C and anti-UNC-68. (D-G) Wild-type body-wall muscle stained with: (D) anti-MYO-B and anti-UNC-68 (bar, 20 μm); (E) anti-MYO-A and anti-UNC-68; (F) anti-vinculin and anti-UNC-68; (G) anti-alpha-actinin and anti-UNC-68. In D-G, views parallel (top) and perpendicular (bottom) to the surface of the animal are shown.

anti-UNC-68 staining is eliminated in *unc-68(r1161)* mutants (Fig. 7B). Myosin heavy chain C (MYO-C) is a pharynx-specific myosin isoform (Moerman and Fire, 1997). Fig. 7C shows a wild-type pharynx stained with anti-UNC-68 (green/yellow) and anti-MYO-C (red) The UNC-68 signal appears closely associated with the MYO-C containing filaments. Fig. 7A and C confirms that UNC-68 staining in pharyngeal muscles is limited to the posterior half of the isthmus ('is', Fig. 7B) and the terminal bulb ('tb', Fig. 7B), and is absent from the corpus ('c', Fig. 7B) and anterior isthmus.

Double-labeling of body-wall muscle with anti-UNC-68 and anti-myofilament lattice proteins (myosin heavy chains A and B, vinculin, and alpha-actinin) shows that UNC-68 is predominantly located in the A-band region, near the apical plasma membrane. The *C. elegans* myofilament lattice is a relatively thin (approx. 1-1.5 μm) structure that extends inward from the plasma membrane (Fig. 8). Myosin heavy chains A and B (MYO-A and MYO-B) are thick filament components whose position marks A-bands (Moerman and Fire, 1997). Vinculin and alpha-actinin are components of dense bodies, the attachment points for thin filaments that are centered in I-bands. Vinculin is located at the base of dense bodies; alpha actinin is located in the portion of dense bodies that project into the muscle cells (Francis and Waterston, 1985; Moerman and Fire, 1997). For each panel of Fig. 7D-G, optical sections that are parallel to the plane of the apical plasma membrane are shown above sections that are perpendicular to the plane of the membrane (lateral views). UNC-68 staining is shown in green, and the myofilament lattice proteins are shown in red.

In combination with anti-MYO-B and anti-MYO-A, the anti-UNC-68 signal overlaps A-bands (see Fig. 7D,E, top). In z-series optical sections, the UNC-68 signal was stronger in sections closer to the plasma membrane than were the anti-MYO-B or anti-MYO-A signals. In combination with anti-alpha-actinin or anti-vinculin, the UNC-68 signal clusters in the A-band region, between the rows of dense bodies (Fig. 7F,G, top). In z-series optical sections, the UNC-68 signal is most strongly co-localized with that of vinculin.

Lateral views confirmed the relative positions of UNC-68 and the four marker proteins. The UNC-68 signal is a relatively thin, punctate band overlying the myofilaments but closer to the apical plasma membrane than either MYO-B (Fig. 7D, bottom) or MYO-A (Fig. 7E, bottom). The punctate UNC-68 signal alternates with the punctate vinculin (Fig. 7F, bottom) and alpha-actinin (Fig. 7G, bottom) signals. We conclude from the double-labeling experiments that the UNC-68 channels are adjacent to the plasma membrane in the A-band region, at a depth comparable to vinculin (Fig. 7F, bottom).

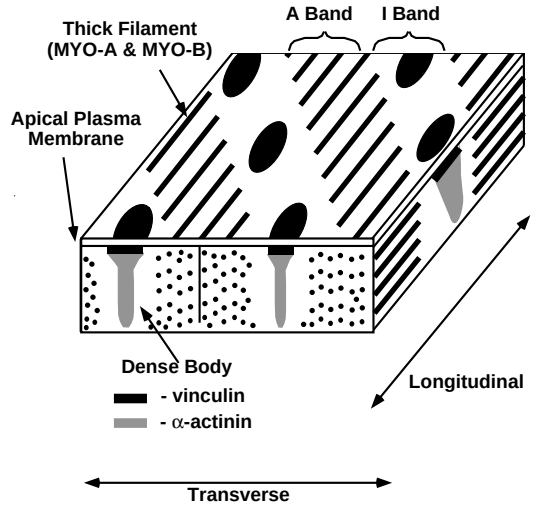

Fig. 8. The *C. elegans* body-wall muscle myofilament lattice. The diagram shows body-wall muscle sarcomeres from longitudinal and transverse perspectives. The cuticle, or outer surface of the animal is connected to the apical plasma membrane (Moerman and Fire, 1997). The relative locations of thick filament myosins (MYO-A and MYO-B) and dense body proteins (vinculin and α-actinin) are shown. Thin filaments are not shown.

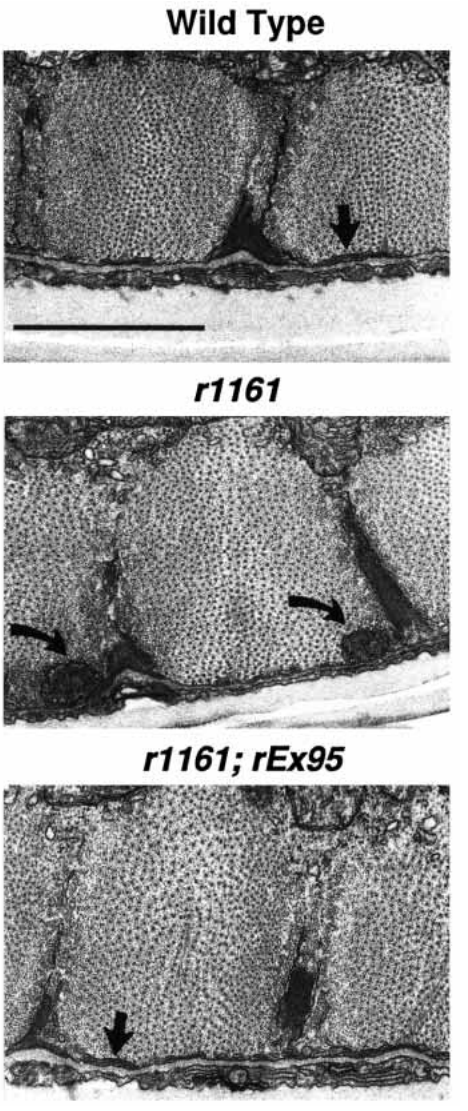

Fig. 9. Transverse sections of body-wall muscle cells in wild type, *unc-68* mutant (*r1161*), and rescued (*r1161; rEx95*) animals. The arrows in the wild-type (top) and rescued (bottom) panels show plasma membrane-associated vesicles in the A-band region. The curved arrows in the middle (*unc-68* mutant) panel show two enlarged, membrane-bound structures near the base of two adjacent dense bodies (finger-like projections). Bar, 1 μm.

Ultrastructure of wild-type and *unc-68* mutant body-wall muscle

We examined the ultrastructure of body-wall muscle cells by electron microscopy of transverse sections of adult animals. In wild type, a series of flattened vesicles surround dense bodies and lay adjacent to the apical plasma membrane beneath the myofilament lattice (Fig. 9, top, enlarged in Fig. 10A). The wild-type vesicles are distributed at random positions between dense bodies. Some vesicles appear continuous between dense bodies and the plasma membrane (Fig. 10E,F). From measurements taken from eight vesicles in six different sections (e.g. Fig. 10A), we estimate that the spacing between the plasma membrane and wild-type vesicles is 12-14 nm. In *unc-68* null mutants, the vesicles adjacent to the plasma membrane are absent. Instead, enlarged, membrane bound, densely-staining structures are observed in the location normally occupied by wild-type vesicles (Fig. 9, middle, Fig. 10C,D). The vesicles surrounding dense bodies appear normal in *unc-68* mutants (Fig. 9, middle; Maryon et al., 1996)). Normal-looking flattened vesicles are restored in *unc-68* null mutants rescued with the wild-type *unc-68* gene (Fig. 9, bottom, Fig. 10B).

Several observations indicate that UNC-68 RyR channels are localized to these flattened, SR-like vesicles adjacent to the apical plasma membrane. First, observation of sarcomeres from wild-type, *unc-68* mutant, and rescued animals showed a strong correlation between the presence of the wild-type flattened vesicles and Unc-68 (+) expression. Among 86 sarcomeres observed in cross section from 7 different wild-type animals, 75 contained flattened vesicles, and none had the aberrant structures. In 97 sarcomeres from 6 *unc-68* mutant animals (4 different alleles), 3 had near-normal vesicles, while 64 contained enlarged, densely staining vesicles like those seen in Fig. 10C,D. In 2 Unc-68 (+) transformants, 32 of 35 sarcomeres contained normal vesicles; and none contained the enlarged vesicles. Second, the position and distribution of flattened vesicles within A-bands adjacent to the plasma membrane agrees well with the position and distribution of the punctate anti-UNC-68 staining described above. Third, the GFP-tagged UNC-68 protein, which rescues the motility defects of *unc-68* mutants, is seen in living body-wall muscle cells as a regular punctate pattern near the apical plasma membrane (Fig. 3B).

DISCUSSION

Our experiments show that UNC-68 RyR channels are

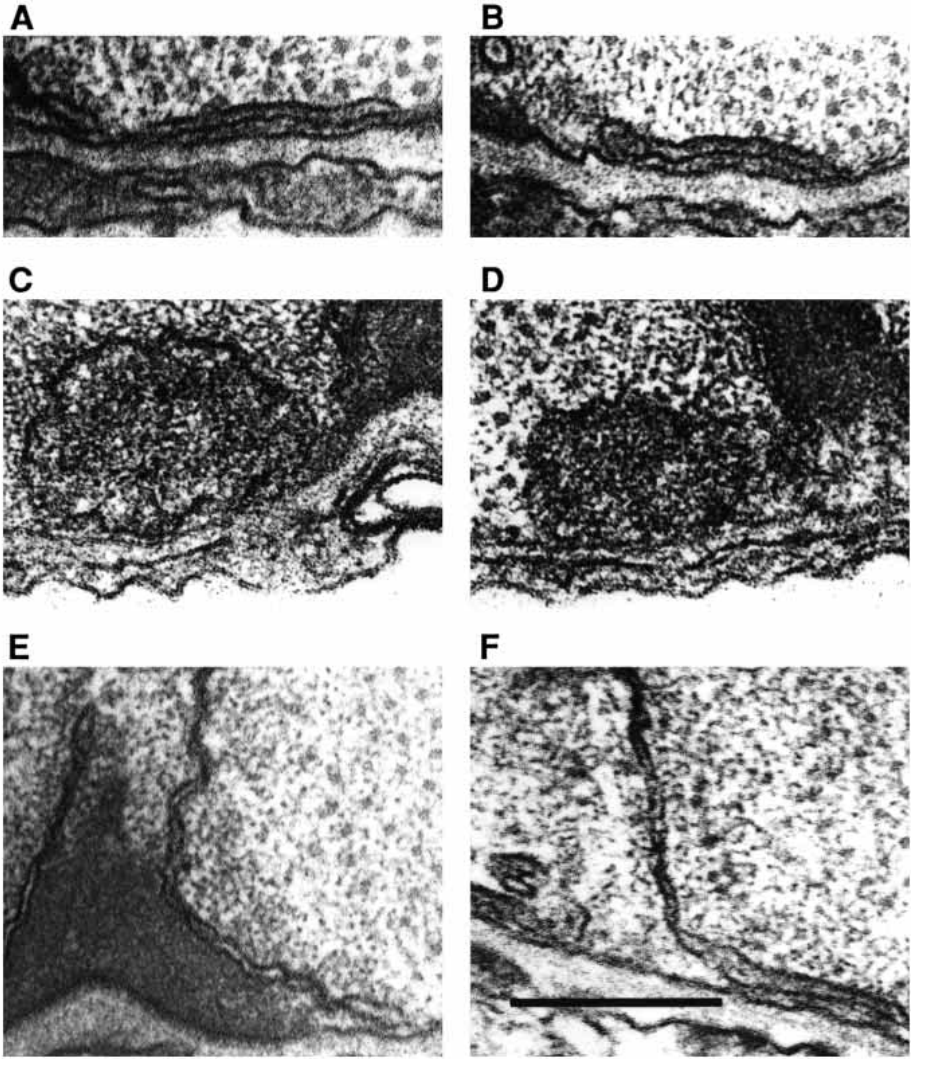

Fig. 10. Enlargements of features shown in A-E of Fig. 9. (A) Normal vesicle (top panel, Fig. 9). (B) Normal vesicle (bottom panel, Fig. 9). (C) Enlarged structure in *unc-68* mutant muscle (left middle panel, Fig. 9). (D) Enlarged structure in *unc-68* mutant muscle (right middle panel, Fig. 9). (E) Vesicle in wild-type continuous with a dense body (top panel left of arrow, see Fig. 9). (F) Vesicle in wild-type continuous with a dense body not shown in Fig.9. Bar, 0.1 μm.

expressed in most muscle cell types in *C. elegans*. Expression of *unc-68* in body-wall muscles is necessary for normal locomotion. Expression of *unc-68* in the posterior muscles of the pharynx appears to be required for wild-type growth rate and brood size. We also observe UNC-68 expression in egg-laying, male tail, and enteric muscles, but the role played by RYRs in these cells is not yet clear.

UNC-68 expression in the pharynx

UNC-68 is expressed in the terminal bulb and isthmus muscle cells of the posterior pharynx. The pharynx consists of (anterior to posterior) the corpus, the isthmus, and the terminal bulb (indicated as c, is and tb, respectively, in Fig. 7B; Albertson and Thomson, 1976). Bacteria are pumped through the lumen of the corpus and isthmus into terminal bulb. The terminal bulb crushes the bacteria and expels the resulting suspension into the gut. Visible defects in pharyngeal pumping in *unc-68* mutants consist of sporadic failures of the anterior isthmus muscles to open during pumping, and of the terminal bulb to relax after a pump (L. Avery and R. Lee, personal communication). The reductions in brood size and growth rate of *unc-68* mutants are attributable to these defects, since other mutations affecting pharyngeal pumping reduce growth rate and fecundity, presumably due to malnourishment, (Avery, 1993; Avery and Thomas, 1997).

Immunolocalization of UNC-68 channels in pharyngeal muscle cells shows a close association with contractile filaments, which consist of radially oriented, single sarcomere myofilaments running between the basal and apical membranes. Contraction of these filaments opens the lumen. Terminal bulb muscles contain both radial and longitudinal myofilaments, whose opposing contractions generate grinding motions (Albertson and Thomson, 1976). The myofilament protein myosin-C (MYO-C) is present in all pharyngeal muscle cells (Moerman and Fire, 1997). As seen in Fig. 7C, UNC-68 staining is co-localized with MYO-C staining. The association of UNC-68 with myosin-containing filaments suggests that a SR may surround the myofilaments in the posterior pharynx. The vacuoles in *unc-68* mutant pharynxes (Fig. 4) are presumably the pharyngeal equivalent of aberrant SR vesicles seen in body-wall muscle (see Figs 9, 10).

The defects of pharyngeal muscle contraction in *unc-68* mutants are not simply explained by a failure to release Ca^{2+} prior to contraction. The isthmus consists of three longitudinal muscle cells (Albertson and Thomson, 1976). Contraction of the anterior and posterior halves of these cells is uncoupled. The contractions (pumping) of corpus, anterior isthmus and terminal bulb muscles are synchronized. In contrast, posterior isthmus muscle contractions occur (after a pump) in about one in four pumps as anterior-posterior peristaltic waves (Avery and Thomas, 1997). The localization of UNC-68 channels to the posterior isthmus (see Figs 6B, 7A,C) suggests that RyRs could be involved in propagating peristaltic contraction waves. Interestingly, the defect observed in *unc-68* mutants is the failure of the *anterior* pharynx to open (i.e. to contract), while peristaltic contractions of the posterior isthmus are grossly normal (L. Avery and R. Lee, personal communication). UNC-68 staining is also intense in terminal bulb muscles (Figs 6B, 7A,C). Since these muscles sometimes fail to relax in *unc-68* mutants, UNC-68 channels could function to repolarize the terminal bulb muscles, as suggested for RyRs in arterial smooth muscle in mammals (Nelson et al., 1995).

UNC-68 expression and localization in body-wall muscle

UNC-68 expression is required in body-wall muscle cells for normal locomotion. Transformation of *unc-68* null mutant animals with the wild-type *unc-68* gene or the wild-type *unc-68* coding sequence fused to the *myo-3* promoter rescued motility defects and sensitivity to ryanodine paralysis (see Fig. 2). *myo-3* is expressed in body-wall muscles, as well as in sex-specific and enteric muscles (the latter muscles do not affect motility). Because certain *unc-68* reporter constructs are expressed in some neurons (Fig. 1B; Sakube et al., 1997), it was possible that motility defects in *unc-68* null mutants were due in whole or in part to the loss of neuronal function. The rescue experiments with the muscle-restricted *myo-3* promoter show that *unc-68* expression in body-wall muscle is sufficient for wild-type motility (Fig. 2). Furthermore, no staining of neurons is observed with anti-UNC-68 antibodies (Figs 6, 7).

Anti-UNC-68 antibodies show that UNC-68 is located between the myofilament lattice and the apical plasma membrane. Double labeling with anti-UNC-68 and antibodies to dense body proteins show that UNC-68 is located primarily between the rows of dense bodies in the A-band region (Fig. 7F,G). Lateral sections show that UNC-68 is near the plasma membrane (Fig. 7D-G). The alignment of the UNC-68 and vinculin signals shown in Fig. 7F (lower panel) shows that UNC-68 is in the same plane as the base of dense bodies, which are anchored to the plasma membrane (see Fig. 8).

Transverse sections of body-wall muscle viewed in the EM indicate that UNC-68 channels are located in the flattened vesicles adjacent to the apical plasma membrane in Unc-68(+) animals (Figs 9, 10). These vesicles were absent in sections from four different null alleles of *unc-68*, but enlarged, densely staining membrane-bound structures are observed in their place (Figs 9, 10). The absence of UNC-68 RyR channels in these mutants could affect the formation, localization, or function of the SR vesicles. For example, *unc-68* mutant vesicles could be enlarged due to their inability to release Ca^{2+}. In the vertebrate SR, much of the stored Ca^{2+} is bound to calsequestrin, a low affinity, high capacity Ca^{2+}-binding protein. The densely-staining material in the enlarged *unc-68* mutant vesicles could be accumulated calsequestrin-like protein.

In mice, skeletal muscle fibers from RyR-1; RyR-3 double mutant embryos also contain enlarged, spherical SR vesicles at triad junctions (Ikemoto et al., 1997). Muscle fibers from single knockout (RyR-1) embryos lack E-C coupling, but still contain relatively normal looking triad junctions (Takeshima et al., 1994; Buck et al., 1997). The RyR-1 single knockout muscle fibers contain functional RyR-3 channels, which are able to release SR Ca^{2+} by CICR (Takeshima et al., 1995). It thus appears that double mutant animals accumulate the ‘bloated’, dense-staining SR vesicles (thought to contain abundant calsequestrin) because there is no remaining calcium conductance pathway from the SR (Ikemoto et al., 1997). The similarity between enlarged junctional vesicles in RyR-1; RyR-3 double mutant mice and the enlarged vesicles in *unc-68* mutants suggest that UNC-68 RyR channels are the major (if

not only) avenue of Ca^{2+}-release from the SR in *C. elegans* body-wall muscle cells.

Conservation of E-C coupling machinery in metazoans

The localization of *C. elegans* RyRs to specific portions of a vesicular network surrounding the myofilament lattice suggests that the general structure of the SR is conserved in metazoans. The surface membrane-associated vesicles are often continuous with vesicles surrounding dense bodies (e.g. Fig. 10E,F). The dense body-associated vesicles do not stain with anti-UNC-68 antibodies (Fig. 7D-G, below), and are not altered in *unc-68* mutants, indicating that they lack RyRs. Skeletal and cardiac SR networks in vertebrates also contain portions devoid of RyRs (Franzini-Armstrong and Protasi, 1997; Carl et al., 1995). RyRs in vertebrate striated muscle cluster at internal couplings with T-tubules and peripheral couplings adjacent to the surface membrane, visible as 'feet' in electron micrographs (Block et al., 1996; Carl et al., 1995). The 12-14 nm gap between the surface and SR vesicle membranes in *C. elegans* is identical to analogous gaps in vertebrate triad junctions (Block et al., 1996; Wagenknecht and Radermacher, 1995), suggesting that UNC-68 RyRs bridge these gaps. Although distinct darkly staining 'feet' structures are not obvious in the gaps between *C. elegans* SR vesicle and surface membranes, in some sections darkened objects are visible in the gaps that resemble 'feet' (see Fig. 10F, right of scale bar).

RyR-independent contraction in *C. elegans*

unc-68 null mutants are defective in locomotion, but still propagate coordinated contraction waves, showing that sufficient Ca^{2+} enters body-wall muscle cells in the absence of RyRs to allow E-C coupling (Maryon et al., 1996). Ca^{2+} could enter the myoplasm through plasma membrane channels or through intracellular Ca^{2+} channels other than RyRs. Two lines of evidence suggest that the source of Ca^{2+} is not intracellular. First, the morphology of the SR vesicles in *unc-68* mutants suggest that RyRs are the primary Ca^{2+}-release pathway from the SR (above), Second, other than RyRs, the only intracellular Ca^{2+} release channels known to regulate muscle contraction are inositol (1,4,5)-trisphosphate receptors (IP3R) (Berridge, 1993). The *C. elegans* genome contains a single IP3R gene designated *lfe-1* (or *itr-1*, see Clandinin et al., 1998). Antibodies to *lfe-1/itr-1* specifically stain the nerve ring, but do not stain the myofilament lattice or show strong staining in body-wall muscle cells (H. Bayliss, personal communication). Gain of function mutations have been isolated in *lfe-1/itr-1* which suppress ovulation defects of *lin-3* mutants (Clandinin et al., 1998). Homozygous *lfe-1/itr-1* animals exhibit wild-type motility, and *lfe-1/itr-1* mutations do not affect the motility of *unc-68* null mutants (T. Clandinin and P. Sternberg, personal communication). Although the null phenotype of *lfe-1/itr-1* is not yet known, the available evidence suggests that IP3Rs are not involved in regulating body-wall muscle contraction.

The attenuated contraction exhibited by *unc-68* null mutants is best explained by entry of Ca^{2+} through VGCCs in the plasma membrane. In striated muscle of invertebrates, it has been established that VGCCs propagate depolarizing action potentials, and that entry of external Ca^{2+} is necessary for E-C coupling (Gainer, 1968; Weisblat et al., 1976; Hagiwara and Byerly, 1981). In *C. elegans*, the *egl-19* locus encodes a VGCC that affects both action potentials and the contractile state of muscle cells (Lee et al., 1997). *egl-19* encodes a homolog of the pore-forming a-1 subunit of vertebrate muscle L-type VGCCs. Like *unc-68*, *egl-19* is expressed in pharyngeal, sex-specific, enteric, and body-wall muscle cells. Strong loss-of-function mutations in *egl-19* are lethal, causing an embryonic arrest phenotype characteristic of genes essential for body-wall muscle function (Williams and Waterston, 1994). Viable *egl-19* alleles fall into two classes: (1) loss-of-function mutations, which cause feeble pharyngeal and body-wall muscle contractions; (2) gain-of-function mutations, which cause hypercontracted body-wall muscle. Intracellular recordings of action potentials in pharyngeal terminal bulb muscles show that the rate of depolarization is slowed in loss-of-function mutants. The feeble contractions of body-wall muscle in these mutants are thus correlated with reduced Ca^{2+} influx during muscle depolarization. In gain-of-function mutants, the plateau phase of the action potential is prolonged, showing that hypercontracted body-wall muscle in these animals is correlated with increased Ca^{2+} entry (Lee et al., 1997).

The phenotypes of *egl-19* mutants suggest that Ca^{2+} entering through VGCCs regulates contraction of *C. elegans* muscle cells. In wild-type animals, external Ca^{2+} would be amplified by further Ca^{2+} release through UNC-68 RyRs (e.g. by CICR). In *unc-68* null mutants, the entering Ca^{2+} would alone be sufficient to elicit attenuated contraction. This is a notable difference between *C. elegans* and vertebrate or crustacean striated muscles. In the latter muscles, external Ca^{2+} entry plays a signaling role, rather than contributing significantly to the generation of tension (Varro et al., 1993; Györke and Palade, 1992; Fabiato, 1983).

We thank Ross Francis, Michelle Hresko, and David Miller for generous gifts of antibodies; Sarah Crittendon, Voula Kodyani, and Judith Kimble for help with microscopy; Andrew Fire for vectors; and Renate Bromberg for help with EM. We thank Leon Avery, Raymond Lee, Howard Bayliss, Tom Clandinin, and Paul Sternberg for communicating unpublished results. This work was supported by an ACS postdoctoral fellowship to E.M. and National Institutes of Health research grant GM30132 to P.A. This is publication # 3522 from the University of Wisconsin-Madison, Laboratory of Genetics.

REFERENCES

Albertson, D. G. and Thomson, J. N. (1997). The pharynx of *Caenorhabditis elegans*. *Philos. Trans. R. Soc. Lond. B Biol. Sci.* **275**, 299-325.

Avery, L. (1993). The genetics of feeding in Caenorhabditis elegans. *Genetics* **133**, 897-917.

Avery, L. and Thomas, J. (1997). Feeding and defecation. In C. elegans *II*. (ed. D. Riddle, T. Blumenthal, B. J. Meyer and J. R. Priess), pp. 679-716. Cold Spring Harbor Laboratory Press, Cold Spring Harbor.

Bennett, D. L., Cheek, T. R., Berridge, M. J., De Smedt, H., Parys, J. B., Missiaen, L. and Bootman, M. D. (1996). Expression and function of ryanodine receptors in nonexcitable cells. *J. Biol. Chem.* **271**, 6356-6362.

Berridge, M. J. (1993). Inositol trisphosphate and calcium signalling. *Nature* **361**, 315-325.

Brenner, S. (1974). The genetics of *Caenorhabditis elegans*. *Genetics* **77**, 71-94.

Bhat, M. B., Zhao, J., Takeshima, H. and Ma, J. (1997). Functional calcium release channel formed by the carboxyl-terminal portion of the ryanodine receptor. *Biophys. J.* **73**, 1329-1336.

Block, B. A., O'Brien, J. and Franck, J. (1996). The role of ryanodine receptor isoforms in the structure and function of the vertebrate triad. *Soc. Gen. Physiologists Series* **51**, 47-65.

Buck, E. D., Nguyen, H. T., Pessah, I. N. and Allen, P. D. (1997). Dyspedic mouse skeletal muscle expresses major elements of the triadic junction but lacks detectable ryanodine receptor protein and function. *J. Biol. Chem*. **272**, 7360-7367.

Callaway, C., Seryshev, A., Wang, J. P., Slavik, K. J., Needleman, D. H., Cantu, C., Wu, J., Jayaraman, T., Marks, A. R. and Hamilton, S. L. (1994). Localization of the high and low affinity ^{3}H-ryanodine binding sites on the skeletal muscle Ca^{2+} release channel. *J. Biol. Chem.* **280**, 15876-15884.

Carl, S. L., Felix, K., Caswell, A. H., Brandt, N. R., Ball, W. J., Vaghy, P. L., Meissner, G. and Ferguson, D. G. (1995). Immunolocalization of sarcolemmal dihydropyridine receptor and sarcoplasmic reticular triadin and ryanodine receptor in rabbit ventricle and atrium. *J. Cell Biol.* **129**, 673-682.

Caterall, W. A. (1991). Excitation-contraction coupling in vertebrae skeletal muscle: a tale of two calcium channels. *Cell* **64**, 871-874.

Chalfie, M., Tu, Y., Euskirchen, G., Ward, W. W. and Prasher, D. C. (1994). Green fluorescent protein as a marker for gene expression. *Science* **263**, 802-805.

Clandinin, T. R., DeMondena, J. A. and Sternberg, P. W. (1998). Inositol trisphosphate mediates a RAS-independent response to LET-23 receptor tyrosine kinase activation in *C. elegans*. *Cell* **92**, 523-533.

Coronado, R., Morrissette, J., Sukhareva, M. and Vaughan, D. M. (1994). Structure and function of ryanodine receptors. *Am. J. Physiol.* **94**, 1485-1504.

Fabiato, A. (1983). Calcium-induced release of calcium from the cardiac sarcplasmic reticulum. *Am. J. Physiol.* **245**, C1-C14.

Fire, A., Harrison, S. W. and Dixon, D. (1990). A modular set of LacZ fusion vectors for studying gene expression in *Caenorhabditis elegans*. *Gene* **93**, 189-198.

Francis, G. R and Waterston, R. H. (1985). Muscle organization in *Caenorhabditis elegan:* localization of proteins implicated in thin filament attachment and I-band organization. *J. Cell Biol.* **101**, 1532-1549.

Franzini-Armstrong, C. and Protasi, F. (1997). Ryanodine receptors of striated muscles: a complex channel capable of multiple interactions. *Physiol. Rev*. **77**, 699-729.

Gainer, H. (1968). The role of calcium in excitation-contraction coupling of lobster muscle. *J. Gen. Physiol.* **52**, 88-110.

Györke, S. and Palade, P. (1992). Calcium-induced calcium release in crayfish skeletal muscle. *J. Physiol.* **457**, 195-210.

Hagiwara, S. and Byerly, L. (1981). Calcium channel. *Annu. Rev. Neurosci.* **4**, 69-125.

Ikemoto, T., Komazaki, S., Takeshima, H., Nishi, M., Noda, T., Iino, M. and Endo, H. (1997). Functional and morphological features from mutant mice lacking both type 1 and type 3 ryanodine receptors. *J. Physiol.* **501**, 305-312.

Kim, Y. K., Valdivia, H. H., Maryon, E. B., Anderson, P. and Coronado, R. (1992). High molecular weight proteins in the nematode *C. elegans* bind ^{3}H-ryanodine and form a large conductance channel. *Biophys. J.* **63**, 1379-1384.

Lee, R. Y. N., Lobel, L., Hnegartner, M., Horvitz, H. R. and Avery, L. (1997). Mutations in the Alpha-1 subunit of an L-type voltage activated calcium channel cause myotonia in Caenorhabditis elegans. *EMBO J.* **16**, 6066-6076.

Maryon, E. B., Coronado, R. and Anderson, P. (1996). *unc-68* encodes a ryanodine receptor involved in regulating *C. elegans* body-wall muscle contraction. *J. Cell Biol*. **134**, 885-893.

Mello, C. and Fire, A. (1995). DNA transformation. In *Methods in Cell Biology*, vol. 48 (ed. H. E. Epstein and D. C. Shakes), pp. 452-482. Academic Press, San Diego, California.

Miller, D. and Shakes, D. (1995). Immunofluorescence microscopy. In *Methods in Cell Biology*, vol. 48 (ed. H. E. Epstein and D. C. Shakes), pp. 364-395. Academic Press, San Diego, California.

Moerman, D. G. and Fire, A. (1997). Muscle: structure, function and development. In C. elegans *II* (ed. D. Riddle, T. Blumenthal, B. J. Meyer and J. R. Priess), pp. 417-470. Cold Spring Harbor Laboratory Press, Cold Spring Harbor, NY.

Muir, S. R. and Sanders, D. (1996). Pharmacology of Ca^{2+} release from red beet microsomes suggests the presence of ryanodine receptor homologs in higher plants. *FEBS Lett*. **395**, 39-42.

Nelson, M. T., Cheng, H., Rupart, M., Santana, L. F., Bonev, A. D., Knot, H. J. and Lederer, W. J. (1995). Relaxation of arterial smooth muscle by calcium sparks. *Science* **270**, 633-636.

Rios, E., Ma, J. and Gonzalez, A. (1991). The mechanical hypothesis of excitation-contraction (EC) coupling in skeletal muscle. *J. Muscle Res. Cell Motil.* **12**, 127-135.

Sakube, Y., Ando, H. and Kagawa, H. (1997). An abnormal ketamine response in mutants defective in the ryanodine receptor gene ryr-1 (*unc-68*) of Caenorhabditis elegans. *J. Mol. Biol.* **267**, 849-864.

Seok, J. H., Xu, L., Kramarcy, N. R., Sealock, R. and Meissner, G. (1992). The 30S lobster skeletal calcium release channel (ryanodine receptor) has functional properties distinct from the mammalian channel proteins. *J. Biol. Chem.* **267**, 15893-15901.

Sutko, J. L. and Airey, J. A. (1996). Ryanodine receptor Ca2+ release channels: does diversity in form equal diversity in function?. *Physiol. Rev.* **76**, 1027-71.

Takeshima, H., Lino, M., Takekura, H., Nishi, M., Kuno, J., Minowa, O., Takano, H. and Noda, T. (1994). Excitation-contraction uncoupling and muscular degeneration in mice lacking functional skeletal muscle ryanodine-receptor gene. *Nature* **369**, 556-559.

Takeshima, H., Yamazawa, T., Ikemoto, T., Takekura, H., Nishi, M., Noda, T. and Iino, M. (1995). Ca(2+)-induced Ca2+ release in myocytes from dyspedic mice lacking the type-1 ryanodine receptor. *EMBO J*. **14**, 2999-3006.

Takeshima, H., Ikemoto, T., Nishi, M., Nishiyama, N., Shimuta, M., Sugutani, Y., Kuno, J., Saito, I., Saito, H., Endo, M., et al. (1996). Generation and characterization of mutant mice lacking ryanodine receptor type 3. *J. Biol. Chem*. **271**, 19649-19652.

Varro, A., Negretti, N., Hester, S. B. and Eisner, D. A. (1993). An estimate of the calcium content of the sarcoplasmic reticulum in rat ventricular myocytes. *Pfflugers Arch.* **423**, 158-160.

Wagenknecht, T. and Radermacher, M. (1995). Three-dimensional architecture of the skeletal muscle ryanodine receptor. *FEBS Lett.* **369**, 43-46.

Weisblat, D. A., Byerly, L. and Russell, R. L. (1976). Ionic mechanisms of electrical activity in somatic muscle of the nematode *Ascaris lumbricoides. J. Comp. Physiol.* **111**, 93-113.

Williams, B. D. and Waterston, R. H. (1994). Genes critical for muscle development and function in Caenorhabditis elegans identified through lethal mutations. *J. Cell Biol*. **124**, 475-490.

Wood, W. B. (1988). The nematode *Caenhorhabditis elegans*. Cold Spring Harbor Laboratory Press, Cold Spring Harbor, NY.